Earthq Eng & Eng Vib (2020) 19: 541-560 **DOI**: https://doi.org/10.1007/s11803-020-0579-5

A 5D simulation method on post-earthquake repair process of buildings based on BIM

Xu Zhen†, Zhang Furong‡, Jin Wei‡, Wu Yingying‡, Qi Mingzhu‡ and Yang Yajun‡

Beijing Key Laboratory of Urban Underground Space Engineering, School of Civil and Resource Engineering, University of Science and Technology Beijing, Beijing 100083, China

Abstract: The post-earthquake repair process of buildings is one of the key components of building seismic resilience. Understanding the details of the repair process in advance will benefit the evaluation and decision making for the seismic resilience of buildings. To this end, a five-dimensional (5D) simulation method on the post-earthquake repair process of buildings is proposed based on building information modeling (BIM), by which the repair activities can be presented in the way associated with a 3D model, time (denoted as the fourth dimension), and the related costs (denoted as the fifth dimension). First, a decision-making model of repair schemes based on the interval index of the possibility degree is created to determine the optimal post-earthquake repair schemes for a damaged building. Subsequently, an algorithm based on separate flow-repetitive process is designed to automatically make the repair schedule on a BIM platform according to the determined repair schemes. Finally, an algorithm of automatic mapping between the components in BIM and their repair schedules is developed, so that a 5D simulation of a post-earthquake repair process can be implemented. A six-story office building is selected as a case study, and the details of the post-earthquake repair process (e.g., the costs of labor, material and equipment over the repair time) are presented by the proposed 5D simulation method. The outcome of this study can be used to evaluate the seismic resilience of buildings and also to facilitate the decision making for seismically resilient buildings by providing the detailed guidance of the repair process.

Keywords: repair process; seismic resilience; 5D simulation; BIM; repair schedule

1 Introduction

The advancement of earthquake engineering research and seismic design codes has helped to improve the seismic performance of buildings and decrease the probability of earthquake-induced building collapse. For example, only 4 buildings collapsed among all 9,974 buildings built between 1985 and 2009 in the 8.8-magnitude Chilean earthquake on February 27, 2010 (Elnashai *et al*., 2010). However, the economic loss reached up to $30.0 billion, accounting for 24.2% of the global reported losses ($123.9 billion) in 2010 (Guha-Sapir *et al*., 2011), which severely affected the post-disaster recovery and made it impossible to satisfy the demand of seismic resilience (Bruneau *et al*., 2003). Therefore, the seismic resilience of buildings deserves more attention and further study.

The post-earthquake repair process of buildings is one of the key components of building seismic resilience. That is why simulating this process is of vital importance to evaluation and decision making for the seismic resilience of buildings. Specifically, detailed information (e.g., the costs and repair time) can be used during the repair process as quantitative indexes for measuring the seismic resilience of a building. Moreover, the simulation of the repair process helps to understand the key process of seismic resilience and to discover the important factors affecting resilience (e.g., the requirements of labor, equipment, and material during the repair process), which will benefit the decision making for building seismic resilience.

However, the existing research on the simulation of the post-earthquake repair process of buildings is very limited. Charalambos *et al*. (2014) determined the damage state, repair cost and time of structural components subject to different intensities of earthquakes, but their work did not involve specific repair schemes and processes. Xiong *et al.* (2020), and Lin and Wang (2017) proposed

Correspondence to: Xu Zhen, Beijing Key Laboratory of Urban Underground Space Engineering, School of Civil and Resource Engineering, University of Science and Technology Beijing, Beijing 100083, China
E-mail: xuzhen@ustb.edu.cn
†Associate Professor; ‡Master Student

Supported by: Scientific Research Fund of Institute of Engineering Mechanics, China Earthquake Administration under Grant No. 2019EEEVL0501, General Program of the National Natural Science Foundation of China under Grant No. 51978049 and Beijing Nova Program of Science and Technology under Grant No. Z191100001119115
Received April 8, 2020; **Accepted** June 6, 2020

the workflows for simulating the repair sequence of buildings after an earthquake on the city and community scale, respectively. Longman and Miles (2019) developed a new simulation modeling programming library to discover the post-earthquake distribution of funds and labors in a community. However, most of the existing research on post-earthquake repair simulation is on the city and community scale, not on the scale of individual buildings. To obtain high-fidelity results related to resilience, the simulation of the post-earthquake repair process must be performed for individual buildings.

An important precondition for simulating the post-earthquake repair process of buildings is to evaluate the level of the seismic damage state of building components, which can be obtained through pre-earthquake prediction or post-earthquake investigation. Currently, many scholars (Hofer *et al.*, 2018; Hu *et al.*, 2010; Powell and Allahabadi, 1988; Xiong *et al.*, 2017; Yue *et al.*, 2016) have proposed high-fidelity methods for seismic damage prediction or post-earthquake investigation. For example, Xu *et al.* (2019) proposed a method of seismic damage prediction based on building information modeling (BIM) and the next-generation performance-based design code (i.e., FEMA P-58), by which the seismic damage of each component can be assessed.

Although the high-fidelity seismic damage of building components can be obtained, the following three challenges need to be addressed for the simulation of post-earthquake repair process of buildings:

(1) How to determine the optimal post-earthquake repair schemes for damaged components. For a certain seismic damage state, a type of component may have dozens of repair schemes, and each scheme has different repair details, such as the costs, repair time, construction complexity, dependence on large equipment, etc. It is particularly difficult to quickly determine the optimal repair schemes according to the seismic damage of a building and the preferences of stakeholders.

(2) How to make a repair schedule automatically. After the repair schemes are determined, the corresponding repair schedule needs to be made. The purpose of the repair schedule is to complete the post-earthquake repair as soon as possible under the condition of limited labor and resources. However, it is complicated and time-consuming to create an optimal repair schedule, because various types of construction processes and lots of parameters on schedule (e.g., working space, repair time, and repair procedures) need to be determined.

(3) How to perform a five-dimensional (5D) simulation of the post-earthquake repair process. The simulation of the repair process not only requires the 3D model of the building to display the repair process in a realistic way, but also needs the information of time (fourth dimension) and cost (fifth dimension) to provide detailed results and discover the potential problems during the repair process. However, the existing research (AbouRizk, 2010; Barazzetti and Banfi, 2017; Goodrum *et al.*,2006; Hilfert and König, 2016; Wang, 2013; Wen, 2015; Xu, 2017; Yun *et al.*, 2014; Zhou *et al.*, 2015) on the 5D simulation of repair process of buildings is very limited now.

For challenge (1), the existing studies (Eid and El-Adaway, 2017; Koliou and Lindt, 2020; Lounis and McAllister, 2016) on how to determine the optimal post-earthquake repair scheme for a damaged building are very few. Eid and El-Adaway (2017) proposed a sustainable decision-making tool for disaster recovery of communities, through integrating the economic vulnerability indicator into the associated stakeholder's objective function, which can better guide the reconstruction work. Lounis and McAllister (2016) presented a framework of risk-informed decision making for the life-cycle performance of infrastructure facilities considering sustainability and resilience, which can aid to make a repair scheme. Koliou and Lindt (2020) quantified building functionality for different building types through the functional fragilities, and predicted the repair time and cost of building types after the disaster, which may be further used in risk-informed decision making. However, these research works did not aim for earthquake disasters. The repair schemes for different disasters have wide gaps. Therefore, a specialized method for determining post-earthquake repair scheme of buildings is necessary.

For challenge (2), many existing research studies (Hamledari *et al.*, 2017; Li *et al.*, 2017; Torres-Calderon *et al.*, 2019) have been performed to automatically make the construction schedule. Nguyen (2005) outlined a framework that can assist construction planners and schedulers in automatically generating sequences of construction activities for a multi-story building based on the deduction of spatial relationships between the building components. Mohammadi *et al.* (2016) automatically presented how the limited resources affect the time and cost of building projects based on the simulation of construction process. Park and Cai (2015) created a matching mechanism between the elements in the BIM model and the work breakdown structure (WBS) of schedule, by which detailed construction schedules can be automatically generated. Tauscher *et al.* (2014) combined BIM and 4D visualization to aid in making the construction schedule. Yeoh *et al.* (2017) utilized a query language to enable project information to be embedded in the construction requirement specification and automatically generate construction schedules. However, the research on the post-earthquake repair schedule of buildings is very limited. The post-earthquake repair schedule of buildings is quite different from the normal construction schedule of new buildings. For example, the repair process generally starts from the removal of severely damaged components, while the construction process generally starts from building a foundation. Therefore, in-depth research on the creation of the repair schedule is necessary.

For challenge (3), the BIM technology can be

widely used for the 5D simulation of the construction process (AbouRizk, 2010; Goodrum *et al.*, 2006). Yun *et al.* (2014) realized the BIM-based simulation of construction process by developing a 3D display platform. Some scholars (Barazzetti and Banfi, 2017; Hilfert and König, 2016; Wang, 2013; Xu, 2017) have combined virtual reality (VR) technology with BIM to achieve highly realistic simulations of the construction process. In order to reduce the uncertainty of project cost during the construction process, a system for precise cost management was built based on the BIM-based 5D simulation of construction process and back-propagation artificial neural network (Wen, 2015; Xu, 2017). An investigation (Zhou *et al.*, 2015) indicates that the simulation of construction process can be used to identify potential issues of construction projects. However, the current research on the 5D simulation of the construction process focuses on buildings to be constructed, rather than on damaged buildings. Therefore, a specialized 5D simulation method for repair process needs to be further investigated.

To address the above three challenges, a 5D simulation method on post-earthquake repair process of buildings based on BIM is proposed in this study, by which the repair activities can be presented in the way associated with the 3D model, time, and the related costs. First, a decision-making model of repair schemes based on the interval index of possibility degree is created, to determine the optimal post-earthquake repair schemes for a damaged building. Subsequently, an algorithm based on separate flow-repetitive process is designed to automatically make the repair schedule on a BIM platform according to the determined repair schemes. Finally, an algorithm of automatic mapping between the components in BIM and their repair schedules is developed, so that a 5D simulation of post-earthquake repair process can be implemented. A six-story office building is selected as a case study, and the details of the post-earthquake repair process (e.g., the costs of labor, materials and equipment over the repair time) are presented by the proposed 5D simulation method.

2 Framework

The framework of the proposed 5D simulation method for post-earthquake repair process of buildings is shown in Fig. 1. It includes three steps:

Step 1: Determine the optimal post-earthquake repair schemes. First, the cost, time, construction complexity, dependence on large equipment, and repair effect are used as evaluation indexes to determine the optimal repair schemes. In addition, interval numbers are adopted considering the uncertainty in evaluation indexes, and thus the interval attribute matrix needs to be constructed to describe attributes of different evaluation indexes. Subsequently, a weight vector combining subjective and objective information is also adopted. Finally, a decision-making model of repair schemes based on the interval index of possibility degree is created, by which the possibility degrees of all the repair schemes are calculated using the interval attribute matrix and the corresponding weight vectors. Consequently, the optimal repair schemes can be determined by the ranking of the possibility degrees.

Step 2: Make a repair schedule automatically. First, separate flow-repetitive construction is adopted to make a repair schedule in this study. Then, the key parameters of the separate flow-repetitive construction (e.g., working space, rhythm and pace) are calculated to determine the details of the repair schedule. Finally, an algorithm for automatically making the repair schedule is designed and developed based on a BIM platform.

Step 3: Produce a 5D simulation of the post-earthquake repair process. First, the BIM model of a building and the corresponding repair schedule are integrated in a simulation platform. Subsequently, an algorithm is created to automatically map the components in BIM and their repair schedules, by using the filtering functions in BIM. Finally, the repair process of buildings is realistically simulated, and the repair details (e.g., the costs of labor, equipment and material) are also dynamically displayed.

To implement the above 5D simulation, some

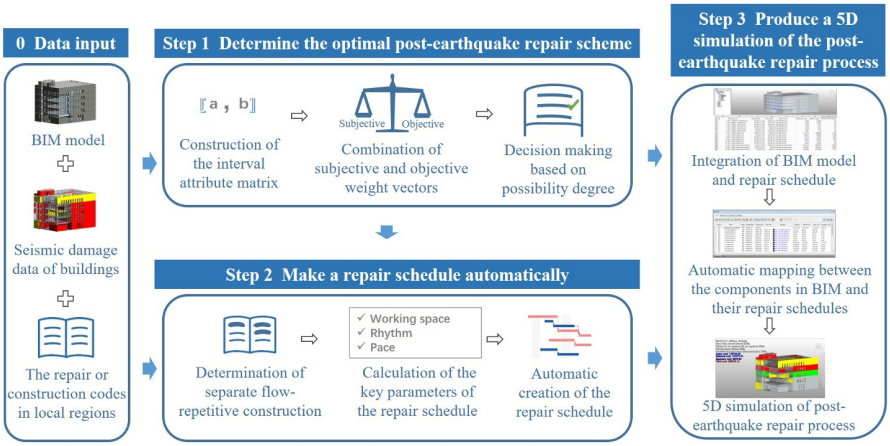

Fig. 1 Framework of this study

data are required in this study. First, the BIM models of buildings are needed, which can be built by Revit, MicroStation, etc. Secondly, the seismic damage data of buildings (i.e., the damage states and repair quantities of all the components) are also necessary, which can be obtained by a prediction method based on BIM and FEMAP-58 (Xu *et al.*, 2019). In detail, the seismic damage of BIM components is calculated by the time-history analysis (THA) and the fragility curves in FEMA P-58, while the accurate repair quantities of components are calculated based on the ontology-based deduction between components. Note that the seismic damage data of each component can also be obtained through field investigation if a building suffers a real earthquake. Thirdly, the repair or construction codes in local regions (such as CSI code (Christodoulou *et al.*, 2010; CSI and CSC, 2016) and the repair code of China (BCHUD, 2012)) are needed to perform a 5D simulation following the local repair rules.

3 Method

3.1 Decision-making model of repair schemes based on the interval index of possibility degree

For a damaged building due to an earthquake, its components can be classified into intact, repairable, and irreparable components according to their seismic damage states and performance criteria (e.g., FEMA P-58) (Xu *et al.*, 2019), and different classes of components have different repair solutions. In detail, there is no need to repair intact components; irreparable components will be removed and rebuilt. For repairable components, various repair schemes are available (BCHUD, 2012). For instance, a beam has more than twenty repair schemes, according to the Beijing repair code for building renovation projects (BCHUD, 2012). Therefore, how to determine the optimal repair schemes is an important problem.

In this study, a decision-making model of repair schemes based on the interval index of possibility degree is proposed to determine the optimal repair schemes. The method of the interval index of possibility degree is a widely-used mathematical model for the multi-attribute decision making problem (Ge *et al.*, 2016; Liu *et al.*, 2018; Wang *et al.*, 2005; Yang *et al.*, 2019), which can fully consider the uncertainties in the process of decision making. In this method, interval indexes are used to quantify the uncertain attributes of evaluation indexes in different schemes, and the possibility degrees that a scheme is better than other schemes are calculated based on the interval indexes. By using the possibility degrees, the schemes can be ranked, and the optimal scheme will be determined. In this study, both the attributes of repair schemes and decision makers' preferences exhibit large uncertainties, thus the method of the interval index of possibility degree is adopted. The proposed decision-making model based on the interval index of possibility degrees includes three steps: constructing the interval attribute matrix, combining weight vectors, and making a decision based on possibility degree, which will be elaborated in the following sections.

3.1.1 Constructing the interval attribute matrix

It is necessary to determine the alternative repair schemes and the interval attributes of the evaluation indexes before constructing the interval attribute matrix.

In this study, all the repair schemes for a type of component are defined as its alternative repair schemes. In order to fully reveal the advantages and disadvantages of the alternative repair schemes, five evaluation indexes are selected, i.e., cost, time, construction complexity, dependence on large equipment, and repair effect, according to the relevant literature (Lin *et al.*, 2008; Lu *et al.*, 2016; Scheuer *et al.*, 2003). Specifically, cost and time are quantitative evaluation indexes, while construction complexity, dependence on large equipment, and repair effect are qualitative evaluation indexes. For the quantitative indexes (i.e., cost and time), although the exact attribute values can be calculated by the repair or construction codes, uncertainty still exists in the repair process, and thus interval numbers are used to indicate the uncertainty of these quantitative indexes. For the qualitative evaluation indexes (i.e., construction complexity, dependence on large equipment and repair effect), the exact attribute values cannot be directly calculated, and thus the interval numbers are also appropriate. These interval numbers can be determined by professionals and experts according to their own experience. In this study, the professional engineers from Aeido Group (2018), an enterprise for the earthquake reinforcement of buildings in China, were invited to score the repair schemes of different components of buildings. Taking a reinforced-concrete (RC) beam for example, the interval numbers of the repair schemes are shown in Table 1.

After the alternative repair schemes and the attribute values of the evaluation indexes are determined, the interval attribute matrix can be constructed. Taking an RC beam as an example, six repair schemes are selected from all the repair schemes in the repair code (BCHUD, 2012), and defined as A_1, A_2, A_3, A_4, A_5 and A_6, respectively. Note that only six repair schemes are selected so as to demonstrate the usage of the proposed method, and that more repair schemes can be considered in the actual calculation. As well, five evaluation indexes (i.e., cost, time, construction complexity, the dependence on large equipment and repair effect) are defined as E_1, E_2, E_3, E_4 and E_5, respectively. The above data on repair schemes and evaluation indexes are shown in Table 2.

According to Table 2, an initial interval attribute matrix $\boldsymbol{D}$ can be constructed, as Eq. (1).

Table 1 Part of interval numbers of repair schemes for an RC beam

Number	Repair scheme		Construction complexity 1-10 (complex-simple)	Dependence on large equipment 1-10 (dependence-independency)	Repair effect 1-10 (bad-good)
1	Enlarge cross-section	Cast-in-place concrete	[5.5-6.5]	[4.5-5.5]	[6.5-7.5]
2		Precast concrete	[7.5-8.5]	[5.5-6.5]	[7.5-8.5]
3	Stiffen with haunch	Cast-in-place concrete	[5.5-6.5]	[4.5-5.5]	[6.5-7.5]
4		Precast concrete	[7.5-8.5]	[5.5-6.5]	[7.5-8.5]
5	Stick steel plate	Double layer, 4 + 4 mm thick	[6.5-7.5]	[4.5-5.5]	[7.5-8.5]
6		U-shaped hoop plate, 4 mm thick	[5.5-6.5]	[4.5-5.5]	[6.5-7.5]

Table 2 Interval attributes of the selected six repair schemes for an RC beam

Alternative repair schemes		A_1	A_2	A_3	A_4	A_5	A_6
Evaluation indexes	E_1	[1200,1260]	[1100,1155]	[1500,1575]	[900,945]	[1300,1365]	[1400,1470]
	E_2	[4,5]	[5,6]	[3,4]	[6,7]	[4,5]	[3,4]
	E_3	[5.5,6.5]	[7.5,8.5]	[5.5,6.5]	[7.5,8.5]	[6.5,7.5]	[5.5,6.5]
	E_4	[4.5,5.5]	[5.5,6.5]	[4.5,5.5]	[5.5,6.5]	[4.5,5.5]	[4.5,5.5]
	E_5	[6.5,7.5]	[7.5,8.5]	[6.5,7.5]	[7.5,8.5]	[7.5,8.5]	[6.5,7.5]

$$\boldsymbol{D}=\begin{bmatrix} [1200,1260] & [1100,1155] & [1500,1575] & [900,945] & [1300,1365] & [1400,1470] \\ [4,5] & [5,6] & [3,4] & [6,7] & [4,5] & [3,4] \\ [5.5,6.5] & [7.5,8.5] & [5.5,6.5] & [7.5,8.5] & [6.5,7.5] & [5.5,6.5] \\ [4.5,5.5] & [5.5,6.5] & [4.5,5.5] & [5.5,6.5] & [4.5,5.5] & [4.5,5.5] \\ [6.5,7.5] & [7.5,8.5] & [6.5,7.5] & [7.5,8.5] & [7.5,8.5] & [6.5,7.5] \end{bmatrix} \tag{1}$$

Assuming that the numbers of evaluation indexes and alternative repair schemes are m and n, respectively, $\boldsymbol{D} = (d_{ij})_{m\times n}$. d_{ij} means the attribute values of evaluation index E_i for the scheme A_j. In detail, $d_{ij} = \left[d_{ij}^{\mathrm{L}}, d_{ij}^{\mathrm{U}}\right]$. d_{ij}^{L} and d_{ij}^{U} are the lower and upper limits of interval attribute values.

Due to the differences in the units of evaluation indexes, the attribute values in matrix $\boldsymbol{D}$ are significantly different, which will affect the accuracy of the decision-making. Therefore, normalization is necessary for matrix $\boldsymbol{D}$. In this study, the evaluation indexes are divided into an expense-based index and a benefit-based index, and different types of indexes have their specialized normalization solutions. Specifically, cost and time are the expense-based indexes, while construction complexity, dependence on large equipment, and repair effect are the benefit-based indexes. Generally, the decision-makers tend to prefer higher benefit-based indexes but lower expense-based indexes. Therefore, the benefit-based indexes are normalized by Eq. (2), while the expense-based indexes are normalized using the reciprocal of d_{ij}, as shown in Eq. (3).

$$r_{ij}^{\mathrm{L}} = d_{ij}^{\mathrm{L}} \Big/ \sqrt{\sum_{j=1}^{n}\left(d_{ij}^{\mathrm{U}}\right)^2}, \; r_{ij}^{\mathrm{U}} = d_{ij}^{\mathrm{U}} \Big/ \sqrt{\sum_{j=1}^{n}\left(d_{ij}^{\mathrm{L}}\right)^2} \tag{2}$$

$$r_{ij}^{\mathrm{L}} = \frac{1}{d_{ij}^{\mathrm{U}}} \Big/ \sqrt{\sum_{j=1}^{n}\left(\frac{1}{d_{ij}^{\mathrm{L}}}\right)^2}, \; r_{ij}^{\mathrm{U}} = \frac{1}{d_{ij}^{\mathrm{L}}} \Big/ \sqrt{\sum_{j=1}^{n}\left(\frac{1}{d_{ij}^{\mathrm{U}}}\right)^2} \tag{3}$$

Through the above normalization, by using Eqs. (2) and (3), the interval attribute matrix $\boldsymbol{D}$ is transformed into $\boldsymbol{R}$, as shown in Eq. (4):

$$\boldsymbol{R}=\begin{bmatrix} [0.383,0.422] & [0.417,0.460] & [0.306,0.337] & [0.510,0.562] & [0.353,0.389] & [0.328,0.362] \\ [0.310,0.497] & [0.259,0.397] & [0.388,0.662] & [0.222,0.331] & [0.310,0.497] & [0.388,0.662] \\ [0.304,0.415] & [0.414,0.542] & [0.304,0.415] & [0.414,0.542] & [0.359,0.479] & [0.304,0.415] \\ [0.314,0.462] & [0.384,0.546] & [0.314,0.462] & [0.384,0.546] & [0.314,0.462] & [0.314,0.462] \\ [0.331,0.436] & [0.382,0.494] & [0.331,0.436] & [0.382,0.494] & [0.382,0.494] & [0.331,0.436] \end{bmatrix} \tag{4}$$

3.1.2 Combining weight vectors

Generally, subjective weights overly empower decision makers' preferences, while objective weights rely too much on sample data (Jahan *et al.*, 2012). In this study, subjective and objective weights are combined. In detail, the interval analytic hierarchy process (IAHP)

(Wu *et al.*, 1995) is used to calculate the subjective weight vector $\boldsymbol{\omega}_1$, while the entropy weight method (EWM) (Wang and Liu, 2019) is used to calculate the objective weight vector $\boldsymbol{\omega}_2$. The comprehensive weight vector $\boldsymbol{\omega}$ can be determined by combining $\boldsymbol{\omega}_1$ and $\boldsymbol{\omega}_2$.

(1) Calculating subjective weight vector by IAHP

In practical engineering projects, decision makers have different preferences for various evaluation indexes. To measure such preferences, the relative importance factors between evaluation indexes are compared by using the numbers from 1 to 9 and their inverses in the traditional AHP. The bigger relative importance factors exhibit the higher preferences of decision makers for the corresponding evaluation indexes. In this study, the IAHP is employed to consider the uncertainty of the relative importance factors by using the interval numbers. Therefore, an interval comparison matrix $\boldsymbol{A}$ can be constructed based on the IAHP. Taking the aforementioned RC beam for example, the matrix $\boldsymbol{A}$ is calculated according to the IAHP for the decision maker, as shown in Eq. (5).

$$\boldsymbol{A}=\begin{bmatrix} [1,1] & [2.833,3.167] & [4.833,5.167] & [5.833,6.167] & [1.833,2.167] \\ [0.316,0.353] & [1,1] & [2.833,3.167] & [3.833,4.167] & [0.462,0.545] \\ [0.194,0.207] & [0.316,0.353] & [1,1] & [1.833,2.167] & [0.240,0.261] \\ [0.162,0.171] & [0.240,0.261] & [0.462,0.545] & [1,1] & [0.194,0.207] \\ [0.462,0.545] & [1.833,2.167] & [3.833,4.167] & [4.833,5.167] & [1,1] \end{bmatrix} \tag{5}$$

where $\boldsymbol{A}=(a_{ij})_{m\times m}$ and $a_{ij}=\left[\underline{a_{ij}},\overline{a_{ij}}\right]$, $1\le i,j\le m$. a_{ij} represents the relative importance interval between the evaluation indexes of E_i and E_j.

The interval eigenvalue method (IEM) (Wu *et al.*, 1995) is used to calculate the weight interval vector of interval comparison matrix. With the assumption of $\boldsymbol{A}=\left[\underline{\boldsymbol{A}},\overline{\boldsymbol{A}}\right]$, the normalized eigenvectors $\underline{\boldsymbol{x}}$ and $\overline{\boldsymbol{x}}$ corresponding to the maximum eigenvalues of matrix $\underline{\boldsymbol{A}}$ and $\overline{\boldsymbol{A}}$ can be calculated, respectively. For the matrix $\boldsymbol{A}$ in Eq. (5), the eigenvectors of $\underline{\boldsymbol{x}}$ and $\overline{\boldsymbol{x}}$ are shown in Eq. (6).

$$\begin{aligned} \underline{\boldsymbol{x}}&=[0.4270,0.1734,0.0764,0.0512,0.2719] \\ \overline{\boldsymbol{x}}&=[0.4266,0.1734,0.0762,0.0500,0.2738] \end{aligned} \tag{6}$$

In the IEM, the parameters of M and N are used to calculate the weight interval vector, as shown in Eq. (7).

$$\boldsymbol{W}=\left[M\underline{\boldsymbol{x}},N\overline{\boldsymbol{x}}\right]=\left(W_1,W_2,\cdots,W_n\right)^{\mathrm{T}} \tag{7}$$

where M and N can be calculated as Eq. (8).

$$M=\sqrt{\sum_{j=1}^{m}\frac{1}{\sum_{i=1}^{m}\overline{a_{ij}}}},\quad N=\sqrt{\sum_{j=1}^{m}\frac{1}{\sum_{i=1}^{m}\underline{a_{ij}}}} \tag{8}$$

By using Eqs. (7) and (8), the interval weight vector corresponding to matrix $\boldsymbol{A}$ is calculated, i.e., $W=\left[[0.4155,0.4334][0.1688,0.1761][0.0744,0.0774]\right.$ $\left.[0.0498,0.0508][0.2646,0.2782]\right]$.

Because the evaluation indexes have no sub-hierarchy in this study, there is no need to combine weights in each hierarchy. In this way, the median value of weight interval vector can be directly defined as the subjective weight vector. For the matrix $\boldsymbol{A}$ in Eq. (5), the subjective weight vector is calculated, i.e., $\boldsymbol{\omega}_1=\left(0.420,0.171,0.075,0.065,0.269\right)^{\mathrm{T}}$.

(2) Calculating objective weight vector by EWM

The EWM (Wang and Liu, 2019) is a commonly-used weighting method that measures dispersion of attribute values. Before calculating the information entropy, it is necessary to preprocess the interval attribute matrix $\boldsymbol{R}$ by using Eq. (9).

$$r_{ij}^{\mathrm{L}}=\frac{r_{ij}^{\mathrm{L}}}{\sum_{j=1}^{n}r_{ij}^{\mathrm{L}}},r_{ij}^{\mathrm{U}}=r_{ij}^{\mathrm{U}}/\sum_{j=1}^{n}r_{ij}^{\mathrm{U}} \tag{9}$$

First, the entropy values corresponding to the upper and lower limits of the interval numbers are calculated as shown in Eq. (10), and then the average entropy values of two limits are adopted as shown in Eq. (11). Finally, the entropy weight of each index is calculated according to Eq. (12).

$$H_i^{\mathrm{L}}=-\frac{1}{\ln(n)}\sum_{j=1}^{n}r_{ij}^{\mathrm{L}}\ln\left(r_{ij}^{\mathrm{L}}\right),H_i^{\mathrm{U}}=-\frac{1}{\ln(n)}\sum_{j=1}^{n}r_{ij}^{\mathrm{U}}\ln\left(r_{ij}^{\mathrm{U}}\right) \tag{10}$$

$$H_i=\left(H_i^{\mathrm{L}}+H_i^{\mathrm{U}}\right)/2 \tag{11}$$

$$\rho_i=\frac{1-H_i}{m-\sum_{i=1}^{m}H_i} \tag{12}$$

For the aforementioned matrix $\boldsymbol{R}$, the corresponding objective weight vector is calculated using ρ_i, i.e., $\boldsymbol{\omega}_2=\left(0.274,0.454,0.159,0.072,0.041\right)^{\mathrm{T}}$.

(3) Combining comprehensive weight vector

The comprehensive weight of the index can be determined by the linear equation, as shown in Eq. (13).

$$\boldsymbol{\omega}=\beta\boldsymbol{\omega}_1+\left(1-\beta\right)\boldsymbol{\omega}_2,\ 0\le\beta\le1 \tag{13}$$

where β can be defined as 0.5 for a well-proportioned combination.

Consequently, the comprehensive attribute values (i.e., z_i) of repair schemes can be calculated by the product of the interval attribute matrix and the comprehensive weight vector, as shown in Eq. (14):

$$z_i = \sum_{i=1}^{m} r_{ij}\omega_i \tag{14}$$

According to Eqs. (13) and (14), the comprehensive weight vector corresponding to the matrix $\boldsymbol{R}$ and the comprehensive attribute of repair schemes can be calculated, respectively, as shown in Eqs. (15) and (16):

$$\boldsymbol{\omega} = (0.347, 0.313, 0.117, 0.068, 0.155) \tag{15}$$

$$z = [[0.338\ 0.449][0.360\ 0.461][0.336\ 0.472] \\ [0.380\ 0.476][0.342\ 0.455][0.343\ 0.480]] \tag{16}$$

3.1.3 Decision making based on possibility degree

Because the comprehensive attribute values of evaluation indexes are expressed in the form of intervals, it is difficult to directly compare the advantages and disadvantages of the repair schemes. Therefore, a decision-making algorithm based on possibility degree (Wan and Dong, 2014; Ye, 2015) is designed to determine the optimal repair schemes.

For the repair schemes a and b, their comprehensive attribute intervals are $a = [a^{\mathrm{L}}, a^{\mathrm{U}}]$ and $b = [b^{\mathrm{L}}, b^{\mathrm{U}}]$, respectively. In this way, define $L(a) = a^{\mathrm{U}} - a^{\mathrm{L}}$ and $L(b) = b^{\mathrm{U}} - b^{\mathrm{L}}$. Then, the possibility degree that a is better than b can be calculated as Eq. (17):

$$p(a \ge b) = \begin{cases} 1 & b^{\mathrm{L}} \le b^{\mathrm{U}} \le a^{\mathrm{L}} \le a^{\mathrm{U}} \\ 1 - \dfrac{(b^{\mathrm{U}} - a^{\mathrm{L}})^2}{2L(a)L(b)} & b^{\mathrm{L}} \le a^{\mathrm{L}} < b^{\mathrm{U}} \le a^{\mathrm{U}} \\ \dfrac{a^{\mathrm{L}} + a^{\mathrm{U}} - 2b^{\mathrm{L}}}{2L(b)} & b^{\mathrm{L}} \le a^{\mathrm{L}} \le a^{\mathrm{U}} < b^{\mathrm{U}} \\ \dfrac{2a^{\mathrm{U}} - b^{\mathrm{L}} - b^{\mathrm{U}}}{2L(a)} & a^{\mathrm{L}} \le b^{\mathrm{L}} \le b^{\mathrm{U}} \le a^{\mathrm{U}} \\ \dfrac{(a^{\mathrm{U}} - b^{\mathrm{L}})^2}{2L(a)L(b)} & a^{\mathrm{L}} < b^{\mathrm{L}} \le a^{\mathrm{U}} \le b^{\mathrm{U}} \\ 0 & a^{\mathrm{L}} < a^{\mathrm{U}} < b^{\mathrm{L}} < b^{\mathrm{U}} \end{cases} \tag{17}$$

Based on Eq. (17), a fuzzy complementary judgement matrix $P = (p_{ij})_{n\times n}$ can be established, where p_{ij} indicates the probability degree that scheme i is better than scheme j. As a result, the ranking vector (i.e., $\boldsymbol{k}$) of the matrix $\boldsymbol{P}$ can be calculated according to Eq. (18), which will be used to determine the best repair scheme.

$$k_i = \frac{1}{n(n-1)}\left(\sum_{j=1}^{n} p_{ij} + \frac{n}{2} - 1\right) \tag{18}$$

Through the above Eqs. (17) and (18), the ranking vector for the six repair scheme of an RC beam is calculated, i.e., $k = (0.144, 0.171, 0.161, 0.199, 0.152, 0.173)$. The maximum value of ranking vector is the fourth element, i.e., 0.199, which means the fourth repair scheme is the best in the six repair schemes of an RC beam. Similarly, the optimal repair schemes of other components can be also determined using the proposed decision-making algorithm based on possibility degree.

3.2 Automatic creation of repair schedule

3.2.1 Selection of construction types

Generally, construction processes can be divided into three types (Lee and Kim, 2014): sequential, parallel and flow construction. Sequential construction is mainly applicable to the projects with insufficient working space and long construction period, while parallel construction is applicable to the projects with sufficient working space and short construction period. For most projects, both working space and construction period are limited, therefore flow construction is widely used, because it can make full use of time and space.

According to the characteristics of rhythm and pace, flow construction can be further classified into different types (Zhu and Song, 2016), as shown in Fig. 2.

In general, the fixed-rhythm flow and the double-rhythm flow are usually applicable to a branch of a project with the same layout in the upper and lower layers. For post-earthquake repair projects, the seismic damage on different floors is quite different, so it is difficult to employ the above two flow construction types. In contrast, there is no layout constraint in the separate flow repetitive construction. In addition, it

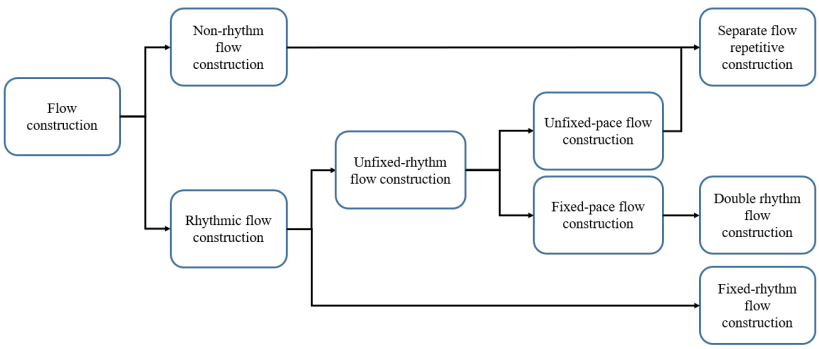

Fig. 2 Classification of flow construction

allows some construction sections to be idle during the construction process, which can be compatible with various engineering objects. Therefore, the separate flow repetitive construction is suitable for post-earthquake repair projects, and the repair schedule is also created based on this type of flow construction in this study.

3.2.2 Parameter determination of separate flow-repetitive construction

To make the schedule of separate flow-repetitive construction, three types of parameters need to be determined, i.e., the parameters of technological process, spatial layout and time arrangement. Specifically, the parameters of technological process are related to the sequence and characteristics of construction process. In this study, the number of repair procedures is only the parameter of technological process, which can be determined by the repair schemes of components.

The parameters of spatial layout mainly include the working space and the number of construction sections and floors. Working space means the necessary activity space required for construction, while construction sections are the executive unit of the project with the same or similar amount of labor, which can be determined by the spatial layout of the project and working space. Generally, working spaces for different components can be obtained according to statistical results such as construction specifications (MOHURD, 2009). Table 3 lists the working spaces of some typical components.

The parameters of time arrangement mainly include rhythm, pace, and repair time. Repair time can be calculated after the rhythm and pace are determined, which will be stated in section 3.2.3. Therefore, the rhythm and pace are critical to make a construction schedule, which will be elaborated as follows.

(1) Rhythm

Rhythm is the time required to complete a certain procedure in a construction section, which can be calculated according to Eq. (19).

$$t_j^i = \frac{Q_j^i H_j^i}{R_j^i N_j^i} \tag{19}$$

where t_j^i is the rhythm for completing construction procedure j in construction section i; Q_j^i is the repair quantity of construction procedure j in construction section i, such as the length and volume of components, which can be obtained through the BIM model (Xu *et al.*, 2019); H_j^i is the labor quota for construction procedure j, which can be obtained for the local construction specifications or codes (MOHURD, 2009); R_j^i means the number of workers for construction procedure j, which is dependent on the available workers and working space; N_j^i is the shift times of workers per day in construction procedure j.

Note that the repair quantities (i.e., Q_j^i) of the correlated parts among the structural components will be calculated following local deduction rules (Xu *et al.*, 2019). For instance, the volume of a column should include its joints, while the volume of a beam should subtract its joints. By doing this, the exact repair quantities of components will be obtained for creating repair schedule.

(2) Pace

Pace is the minimum time interval between adjacent construction procedures. The Pantkovsky method (Yu and Zheng, 2004) is adopted for calculating pace.

First, the total number of rhythms of each construction procedure in each construction section is calculated, according to Eq. (20).

$$a_{i,j} = \sum_{i=1}^{m} t_j^i \ (1 \le j \le n;\ i \le m) \tag{20}$$

where m is the number of construction sections; n is the number of construction layers, which is equal to the floor number of a building; $a_{i,j}$ is the ith accumulation number of the jth construction procedure.

Subsequently, the difference array between adjacent construction procedures is calculated according to Eq. (21).

$$\Delta a_{j,j+1}^i = a_{j,i} - a_{j+1,i-1} \ (1 \le j \le n;\ i \le m) \tag{21}$$

where $\Delta a_{j,j+1}^i$ the ith element of the difference array; $a_{j,i}$ is the ith value of the cumulative number j, while $a_{j+1,i-1}$ is the (i-1)th value of the cumulative number j+1.

Finally, the pace between two adjacent construction procedures can be calculated, according to Eq. (22).

$$K_{j,j+1} = \max\left(\Delta a_{j,j+1}^i\right) (1 \le j \le n-1; i \le m) \tag{22}$$

where $K_{j,j+1}$ is the pace between construction procedures j and j+1.

Table 3 Working spaces of some typical components

Component	Working space
Masonry wall	8.5 m/person
Cast-in-place column	2.5 m^3/person
Cast-in-place beam	3.2 m^3/person
Cast-in-place floor	5.3 m^3/person

3.2.3 Automatic creation of repair schedule

The algorithm for creating the repair schedule is shown in Fig. 3. The numbers of repair procedures and floors are assumed to be *Num_procedure* and *Num_floor*, respectively. Three 2D arrays (i.e., *startTime*[*i*,*j*], *endTime* [*i*,*j*] and *rhythm*[*i*,*j*]) are created to store the start time, end time and rhythm of the *i*th repair procedure on the *j*th floor, and an array (*pace*[*i*]) is also created to store the pace between the *i*th and (*i*+1)th repair procedures.

First, the start time of the repair schedule (i.e., *startTime*[0,0]) is determined by the start time of the first procedure. Subsequently, the repair procedures are performed in sequence according to the repair schedule based on separate flow repetitive construction. Therefore, the start time of the next procedure is equal to the sum of the start time of current procedure and its pace, i.e., *startTime*[*i*+1,*j*] = *startTime*[*i*,*j*] + *pace*[*i*]. For a multi-floor building, each repair procedure will be performed floor by floor. In this way, the end time of a procedure on the current floor is equal to the sum of its start time and rhythm (i.e., *endTime*[*i*,*j*] = *startTime*[*i*,*j*] + rhythm[*i*,*j*]), which is also equal to the start time on the next floor (i.e., *startTime*[*i*,*j*+1] = *endTime*[*i*,*j*]). Finally, the above steps are repeated until the start and end time of all the procedures are calculated, so that the repair schedule is determined.

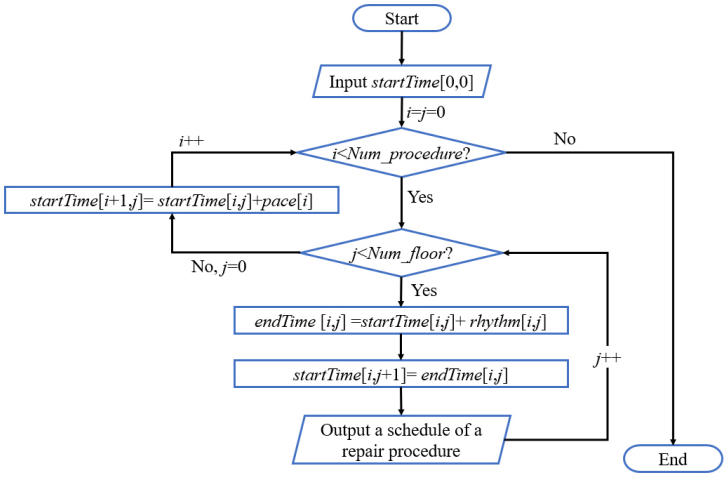

Fig. 3 Algorithm for creating repair schedule

The above algorithm is developed in the Revit API, because Revit is widely-used in BIM modeling. The core code for automating the creation of repair schedule is shown in Fig. 4. In Revit API, the *AddDays*() function is used to update the start and end time of different procedures according to the designed algorithm. In addition, the ID, name, start time, end time, task type, labor cost, material cost and equipment cost of each procedure will be automatically output to form a complete repair schedule.

3.3 5D simulation of post-earthquake repair process

In 5D simulations of post-earthquake repair process, the 3D BIM model, repair time (4D) and repair cost (5D) are the most elemental data. The total repair time of a building and the specific repair time of the damaged components are defined in the repair schedule, which can be automatically created by the aforementioned

```
for (int j= 0; j < Num_floor; j++)
{
    // When the time required for the procedure on the jth floor is non-zero, execute the following statement.
    if (rhythm[i,j] != 0)
    {
        // The end time of the procedure on the jth floor(endTime [i,j]) is equal to the start time of the procedure on the jth floor (startTime[i,j]) plus the flowing rhythm (rhythm[i,j]).
        endTime[i,j] =startTime[i,j].AddDays(rhythm[i,j]) ;
        // The start time of the procedure on the next floor (startTime[i,j+1]) is equal to the end time of the procedure on the jth floor(endTime [i,j])
        startTime[i,j+1]= endTime[i,j];
        // Add the procedure ID, name, start time, end time, task type, labor cost, material cost and equipment cost to the output file named "repairPlan".
        repairPlan += repairItemID + ",F" + (j+1) + Name[repairItemID] + startTime[i,j].ToString("d") + "," + endTime[i,j].ToString("d") + ", "+ Task_type[repairItemID] + repairCost[0,j] + "," + repairCost[1,j] + "," + repairCost[2,j] + "\r\n";
        repairItemID++;
    }
}
```

Fig. 4 Code segment for automatic creation of repair schedule

algorithm in Revit API. In the repair schedule, the repair process of each damaged component is divided into some procedures according to its repair scheme. The total repair cost of a building is equal to the sum of the costs of all the damaged components, while the repair cost of a component is equal to the sum of the costs of all the procedures. Furthermore, the total cost of a procedure is composed of material, labor and equipment costs, which can be calculated as Eqs. (23–26).

$$\text{Total\_cost} = \text{Material\_cost} + \text{Labor\_cost} + \text{Equipment\_cost} \tag{23}$$

$$\text{Material\_cost} = Q_j^i C_1 \tag{24}$$

$$\text{Labor\_cost} = t_j^i R_j^i C_2 \tag{25}$$

$$\text{Equipment\_cost} = Q_j^i C_3 \tag{26}$$

where Q_j^i is the repair quantity of construction procedure j in construction section i in the repair schedule; t_j^i is the rhythm for completing construction procedure j in construction section i; R_j^i means the number of workers for construction procedure j in construction section i; C_1, C_2 and C_3 are the unit material, labor and equipment costs, respectively, which can be obtained from the repair or construction codes in local regions (such as CSI code (Christodoulou *et al.*, 2010; CSI and CSC, 2016) and the repair code of China (BCHUD, 2012)).

After the data of the 3D BIM model, repair time and repair cost are obtained, the workflow of 5D simulation of post-earthquake repair process includes three steps: (1) data integration of BIM and repair schedule; (2) automatic mapping between the components and their repair procedures; (3) implementation of 5D simulation of repair process.

3.3.1 Data integration of BIM and repair schedule

Before the simulation of repair process, the data of BIM and repair schedule need to be integrated in a platform. In this study, Navisworks (Kalyan *et al.*, 2016), a BIM model review software, is selected for data integration. This is because Navisworks can be completely compatible with the BIM model created by Revit and is widely used for construction process simulation.

By using Revit, the BIM model is exported to *.nwc format, which can be directly imported by Navisworks. Besides, the repair schedule can be stored in *.csv format according to the requirements of Navisworks, and then Navisworks will import the whole schedule by the *.csv file. Through the above solutions, the BIM model and the repair schedule can be easily integrated in Navisworks.

3.3.2 Automatic mapping between components and their repair procedures

After the data integration of BIM and the repair schedule, how to map the components in BIM model and their procedures in the schedule is a critical problem. Generally, such mapping is completed manually, which is time-consuming and labor-intensive. To solve this problem, a solution for automatic mapping between the components and their procedures is proposed.

The proposed solution includes two key steps: (1) automatic generation of component sets; (2) automatic mapping component sets and the corresponding procedures. Note that a repair procedure generally involves a set of components. For example, the procedure of wall removal means the walls in severe damage on a floor will be removed. Therefore, the component sets need to be generated according to the corresponding procedures.

(1) Automatic generation of component sets

In this study, an algorithm for automatic generation of component search set is designed based on Revit, by which a search set file can be exported. By importing the search set file, the component sets corresponding to the procedures can be automatically created in Navisworks.

The generation process of the search sets is shown in Fig. 5. First, the component categories and damage states required in the *i*th procedure are obtained. Subsequently, the components are filtered according to the required categories and damage states. Finally, the filtered components are defined as a search set, and their IDs are output for automatic generation of the component set. The above steps are repeated until the search sets for all procedures are formed.

The core code on the generation of search sets is shown in Fig. 6. The class *ElementCategoryFilter* in Revit API is used to filter the components according to the categories and damage states corresponding to the procedures. Through the above code, an *.xml file including the procedure names and corresponding component IDs is output, and then such file is imported into Navisworks to automatically generate component

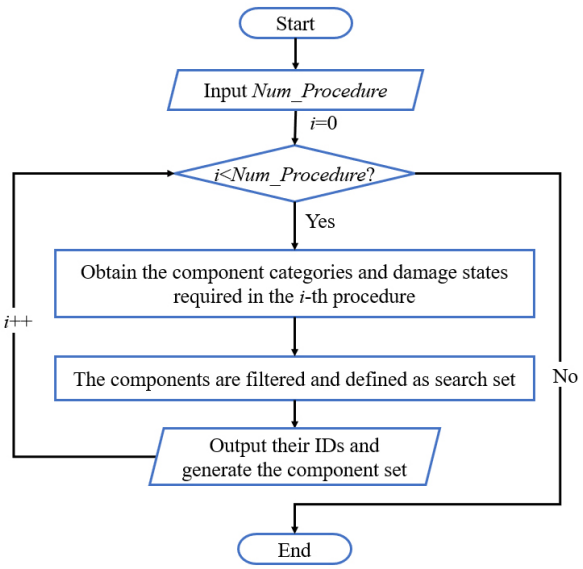

Fig. 5 Generation process of search sets

```
// Obtain the component categories required in the i^th procedure.
ElementCategoryFilter structuralBeamFilter = new
ElementCategoryFilter(BuiltInCategory.OST_StructuralFraming);
unlevelElementCollector.WherePasses(structuralBeamFilter);
IList<Element> elementBeam = (from el in unlevelElementCollector where
el.get_Parameter(BuiltInParameter.INSTANCE_REFERENCE_LEVEL_PARAM).AsVal
ueString() == upLevelName select el).ToList();
foreach (Element element in elementBeam)
  {// Obtain the damage states required in the i^th procedure.
    IList<Parameter> list_P_State = element.GetParameters("P_ damage states ");
    Parameter param_P_State = list_P_State[0];
  // Add ID to the corresponding search set
    if (param_P_State.AsString() == "DS1" || param_P_State.AsString() == "DS2")
    {elementIDs_1.Add(element.Id);}
    else if (param_P_State.AsString() == "DS3")
    {elementIDs_2.Add(element.Id);}
  }
//All the filtered components are defined as search set and their IDs are output for automatic generation of
component sets.
SelectionSet(elementIDs_1, levelName, "Beam- Strengthen ");
SelectionSet(elementIDs_2, levelName, " Beam - Remove ");
SelectionSet(elementIDs_2, levelName, " Beam - Rebuild ");
```

Fig. 6 Code segment for automatic generation of component search sets

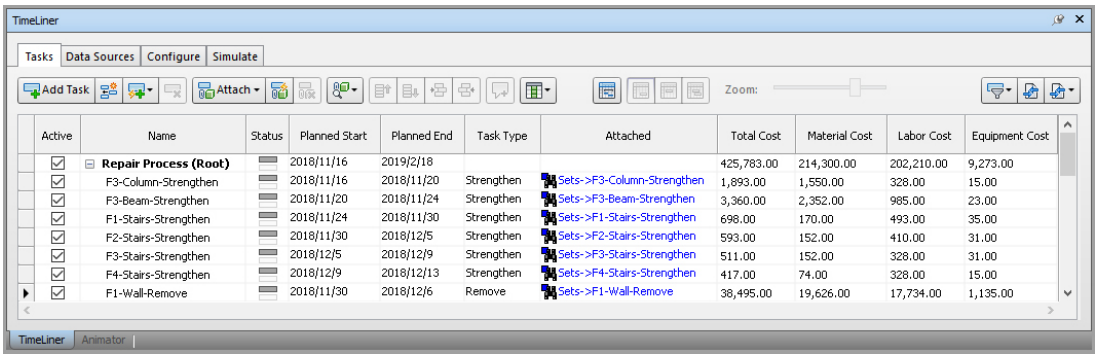

Fig. 7 Automatic mapping between the component sets and their repair procedures

sets corresponding to procedures.

(2) Automatic mapping component sets and the corresponding procedures

If the names of the component sets and the procedures are the same, the component sets will be automatically mapped with their repair procedures by Navisworks. As shown in Fig. 7, the tasks (i.e., repair procedures) have the same name with the sets (blue words in Fig. 7), thus each task is automatically attached with the components in the corresponding sets, which saves lots of manual mapping workloads.

3.3.3 Implementation of 5D simulation of repair process

To implement 5D simulation of post-earthquake repair process, a plug-in named "5D simulation of repair process" is developed in Revit, to provide the necessary data of the schedule and search sets, as shown in Fig. 8. Through the developed plug-in, the start time of the

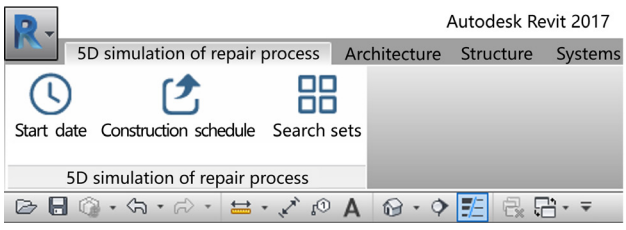

Fig. 8 Plug-in of "5D simulation of repair process"

repair process can be defined and the detailed repair schedule (including the ID, name, start time, end time, task type, labor cost, material cost and equipment cost of each pair procedure) is automatically created in the *.csv format for Navisworks, while the search sets for the corresponding procedures are also output for the following 5D simulation in Navisworks.

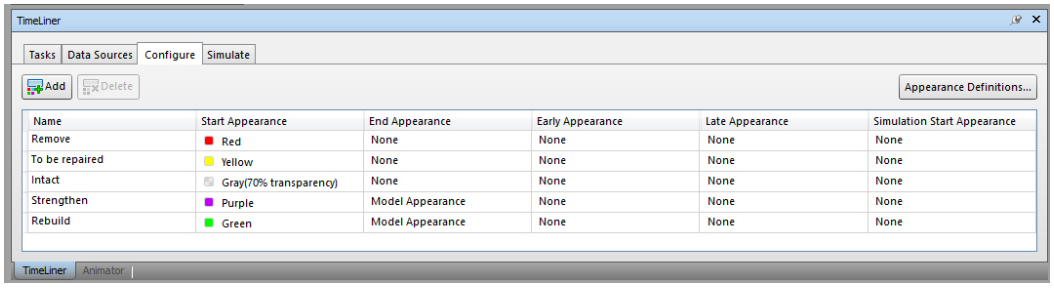

Fig. 9 Configuration of display status for different task types

```
%x%a  $DAYDays  $WEEKWeeks$COLOR_BLACK
$TASKS$COLOR_BLACK
Labor cost: $LABOR_COST$COLOR_BLUE
Material cost: $MATERIAL_COST$COLOR_BLUE
Equipment cost: $EQUIPMENT_COST$COLOR_BLUE
Total cost: $TOTAL_COST$COLOR_RED
```

Fig. 10 Script code for cost display

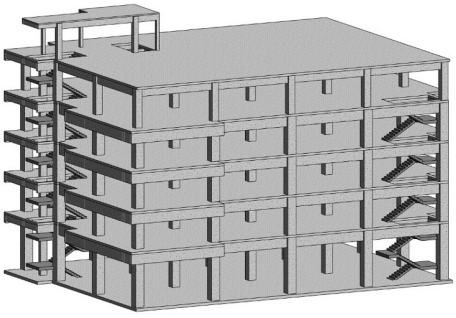

Fig. 11 Structural BIM model

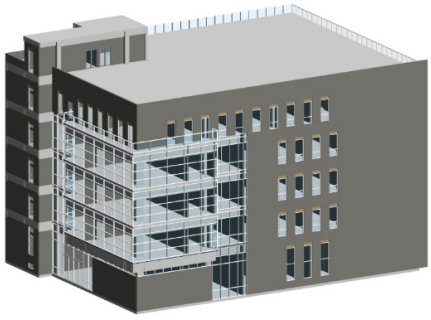

Fig. 12 Architectural BIM model

After the mapping between the component sets and procedures in Navisworks, two preconditioning jobs on visualization need be performed for a 5D simulation of post-earthquake repair process.

In order to highlight these task types during 5D simulation, display states of different task types need to be configured. As shown in Fig. 9, the intact components are displayed in translucent mode, while the components to be repaired, removed, rebuild and strengthened are displayed in yellow, red, green, and purple, respectively. When the repair is completed, the original appearance of the model is recovered.

In order to display the related costs during 5D simulation, the script code is added in Navisworks, as shown in Fig. 10. In detail, "%x%a" in the script is used to show the simulation time, and "$TASKS" will shows the names of procedure. Besides, "$LABOR_COST", "$MATERIAL_COST", "$EQUIPMENT_COST" and "$TOTAL_COST" are used to present the labor, material, equipment and total costs, respectively.

After the above preconditioning jobs are completed, the 5D simulation of post-earthquake repair process can be implemented by using the function of "Timeliner", which will be presented in the Case Study section below.

4 Case study

4.1 Introduction of case study

An office building in Beijing, China was selected as a case study, which is an RC frame structure with 6 floors and a total height of 25.6 m. It covers an approximately rectangular area of 921 m^2 with a length of 33.6 m and a width of 25.2 m. The structural and architectural models with a total of 3,421 components were established using Revit, as a shown in Figs. 11 and 12.

The El-Centro ground motion with a peak ground acceleration (PGA) of 400 cm/s^2 was selected for predicting the seismic damage of a building. Through nonlinear time history analysis, the engineering demand parameters (EDPs) of this building were obtained, as shown in Table 4.

Based on the EDPs in Table 4 and the vulnerability curves in FEMA P-58, the seismic damages of components were calculated (Xu *et al.*, 2019), as illustrated in Fig. 13. The repair process of this damaged building will be simulated using the proposed method in this study.

4.2 Determination of the optimal post-earthquake repair schemes

On one hand, the irreparable components need to be removed and rebuilt. First, the unit cost and time to replace the different types of components can be obtained from

Table 4 The EDPs for the office building

Story	Inter-story drift ratios (rad)		Peak floor accelerations (g)	
	X direction	*Y* direction	*X* direction	*Y* direction
1	0.0032	0.0029	0.6606	0.4895
2	0.0048	0.0033	0.7825	0.6138
3	0.0055	0.0028	0.7259	0.5987
4	0.0057	0.0021	0.7665	0.6358
5	0.0020	0.0018	0.8911	0.6749
6	0.0037	0.0031	1.0218	0.7561

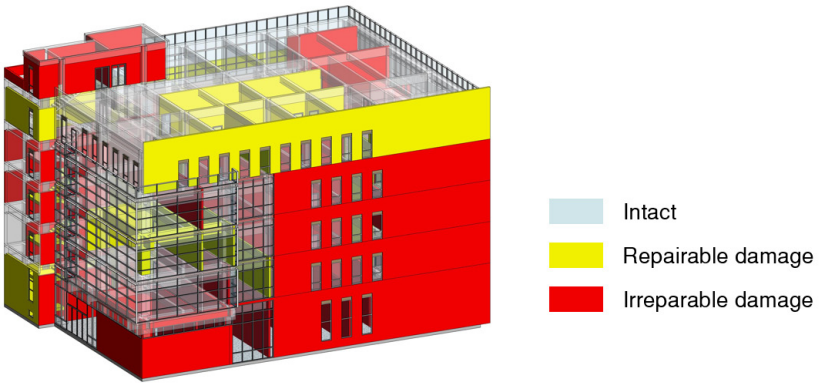

Fig. 13 Seismic damage of all the components

the repair or construction codes in local regions (such as CSI code (Christodoulou *et al.*, 2010; CSI and CSC, 2016) and the repair code (BCHUD, 2012) in China). Subsequently, the repair quantities (e.g., volumes and lengths) of the irreparable components were obtained from the BIM model. Finally, the repair cost and time of these components were calculated by multiplying the unit values and repair quantities. On the other hand, the repairable components (e.g., beams, columns and stairs in this case study) need to be repaired. However, there are too many repair schemes for different components according to the repair code (BCHUD, 2012) in China. Therefore, the proposed decision-making model based on the interval index of possibility degree was adopted to determine the optimal repair schemes for repairable components.

As mentioned before, five indexes (i.e., cost, time, construction complexity, dependence on large equipment and repair effect) were selected for decision making. The values of cost and time for different schemes were obtained by the repair code (BCHUD, 2012). Considering the uncertainty in the repair process, the range within ±5% of the cost and time were used as interval numbers. In addition, professional engineers from Aeido Group (2018), an enterprise for the earthquake reinforcement of buildings in China, were invited to provide interval numbers for the construction complexity, dependence on large equipment and repair effect of each scheme.

Considering the subjective and objective index weights, the possibility degrees of different schemes were calculated and ranked using the proposed method. The optimal repair schemes were determined for the damaged components, as shown in Table 5. Note that the optimal repair schemes listed in Table 5 are either cost-optimized or time-optimized, but a comprehensive result combined with subjective and objective weights. In this study, the subjective weight vector is $\boldsymbol{\omega}_1 = (0.420, 0.171, 0.075, 0.065, 0.269)^{\mathrm{T}}$, which indicates that repair cost is the important factor for decision makers. Taking columns, for example, the objective weight vector is $\boldsymbol{\omega}_2 = (0.527, 0.383, 0.024, 0.056, 0.010)^{\mathrm{T}}$, which indicates the attribute differentiation in repair cost index is the greatest. By combining the subjective and objective weights, the comprehensive weight is $\boldsymbol{\omega} = (0.474, 0.277, 0.049, 0.060, 0.139)^{\mathrm{T}}$. This shows that the weight of repair cost is the greatest, thus the repair scheme for columns in Table 5 tends to be cost-optimized, but is a comprehensive result combined with subjective and objective weights.

4.3 Automatic creation of repair schedule

Using the plug-in of "5D simulation of repair process" developed in this study, the parameters of the separate flow-repetitive construction was calculated and therefore the detailed repair schedule was created

automatically. For example, the part of repair schedule is also demonstrated in Table 6. The creation of the repair schedule took only 10 seconds using the plug-in developed in this study, which can save much manual work.

4.4 5D simulation of post-earthquake repair process

The BIM model and the repair schedule were integrated in Navisworks by the *.nwc and *.csv formats, respectively, as shown in Fig. 14. The search sets were created through the plug-in developed in Revit. By importing the search sets into Navisworks, the component sets were automatically created and mapped with the corresponding repair procedures, as shown in the task panel of Fig. 14. It is worth noting that component mapping is the most time-consuming task for 5D simulation. For the building in the case study, it is estimated that it would take at least 3 hours to map the components and the schedules manually, while it only took 1 minute through the proposed method. Therefore, the proposed method in this study is highly efficiency in application.

After completing the preconditioning jobs on visualization, the 5D simulation of the repair process was performed, as shown in Fig. 15. The upper left corner displays the current time, procedure and detailed costs, and the real-time status of each component is dynamically visualized in the 3D view area. Fig. 16 shows the different states in the repair process, from which the detailed repair progress of the building can be intuitively observed.

4.5 Discussions

In order to compare the repair schemes by the proposed method (denoted as repair scheme A), another group of repair schemes (denoted as repair scheme B) was selected. The research on how to determine post-earthquake repair schemes for damaged buildings is very limited, so professional engineers from Aeido Group recommended repair scheme B based on their traditional experience in this study, as shown in Table 7.

Using the plug-in of "5D simulation of repair process" developed in this study, the detailed repair schedule was created automatically, as demonstrated in Table 8.

Through the proposed method of 5D simulation of

Table 5 Optimal repair schemes for different components

Component category	Seismic damage state	Repair schemes
Walls	Irreparable	Remove and rebuild
	Repairable	Pressure grouting for cracks - Polymer of polyvinyl alcohol solution and cement mortar
Beams	Repairable	Strengthened with carbon fiber reinforced polymer (CFRP)
Floors	Repairable	Strengthened with CFRP
Columns	Repairable	Strengthened with CFRP
Stairs	Repairable	Concrete crack repair techniques

Table 6 Part of the created repair schedule

ID	Procedure	Start time	End time	Task type	Labor cost (CNY)	Material cost (CNY)	Equipment cost (CNY)
0	F3-Column-Strengthen	2018/11/16	2018/11/20	Strengthen	328	1550	15
1	F3-Beam-Strengthen	2018/11/20	2018/11/24	Strengthen	985	2352	23
2	F1-Stairs-Strengthen	2018/11/24	2018/11/30	Strengthen	493	170	35
3	F2-Stairs-Strengthen	2018/11/30	2018/12/5	Strengthen	410	152	31
…	…	…	…	…	…	…	…
20	F3-Wall-Strengthen	2019/2/2	2019/2/7	Strengthen	5747	5466	243
21	F4-Wall-Strengthen	2019/2/7	2019/2/12	Strengthen	3284	3027	134
22	F5-Wall-Strengthen	2019/2/12	2019/2/17	Strengthen	6978	6618	294
23	F6-Wall-Strengthen	2019/2/17	2019/2/18	Strengthen	82	74	3
Total		2018/11/16	2019/2/18	——	202210	214300	9273

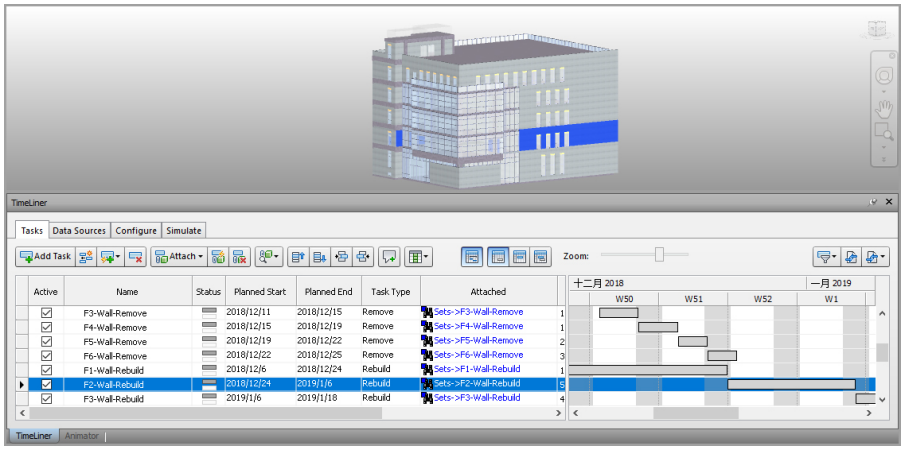

Fig. 14 Automatic mapping between the components in BIM and their repair schedules

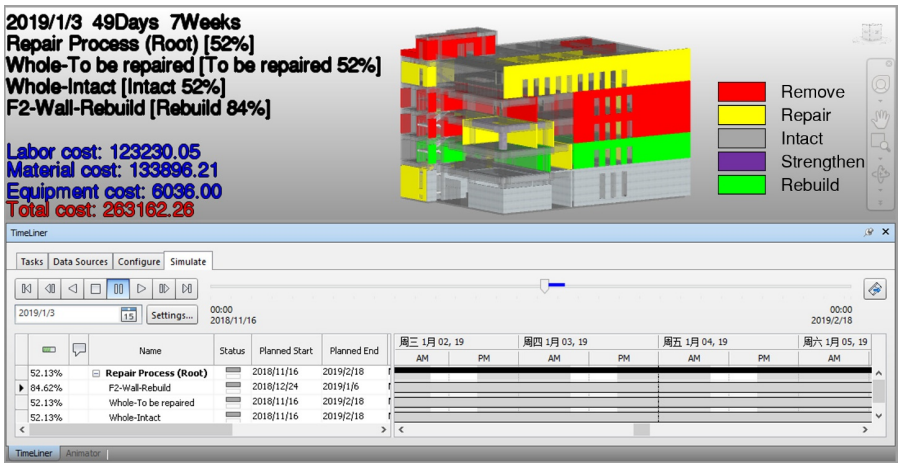

Fig. 15 5D simulation of post-earthquake repair process

the repair process, the detailed repair cost and time of the repair scheme B were obtained, as shown in Table 9. The repair cost and time of the repair scheme A are also demonstrated in Table 9.

It can be observed from Table 10 that the total repair costs of repair schemes A and B are 425,783 CNY and 485,280 CNY, respectively, which indicates that the proposed method saved 12.26% of the total cost compared with repair scheme B. On the other hand, the repair time of the two schemes is almost the same.

In this case study, the proportion of reparable components in all the damaged components is only close to a quarter, thus the total repair cost and time are mainly dominated by the procedures to remove and rebuild irreparable components, which have nothing to do with repair schemes. If only repairable components are compared, the costs of the repair schemes A and B are 57,151 CNY and 116,648 CNY, respectively, as shown in Fig. 17. In that case, the proposed method saved 51% of the cost of repair scheme B. The repair time of repairable components in the repair schemes A and B are 54 days and 60 days, respectively, as shown in Fig. 18. The proposed method also saved 10% of the time of repair scheme B.

Previous study (Xu *et al.*, 2019) have shown that the total repair cost of the same building with the same seismic damage is 463,728 CNY without the optimization of the repair schemes. Because the repair cost is more of a concern when choosing repair schemes, the proposed method saved 8.18% of the total cost compared to the previous study.

Table 7 Repair scheme B for different components

Component category	Seismic damage state	Repair schemes
Walls	Irreparable	Remove and rebuild
	Repairable	Pressure grouting for cracks - Mortar grouting
Beams	Repairable	Stick steel plates
Floors	Repairable	Add composite layer on top of slab
Columns	Repairable	Stick steel plates
Stairs	Repairable	Concrete crack repair techniques

Table 8 Part of the repair schedule for repair scheme B

ID	Procedure	Start time	End time	Task type	Labor cost (CNY)	Material cost (CNY)	Equipment cost (CNY)
0	F3-Column-Strengthen	2018/11/16	2018/11/20	Strengthen	1642	5946	93
1	F3-Beam-Strengthen	2018/11/20	2018/11/24	Strengthen	12151	32216	447
2	F1-Stairs-Strengthen	2018/11/24	2018/11/30	Strengthen	985	170	35
3	F2-Stairs-Strengthen	2018/11/30	2018/12/5	Strengthen	821	152	31
…	…	…	…	…	…	…	…
20	F3-Wall-Strengthen	2019/1/30	2019/2/5	Strengthen	6896	6693	243
21	F4-Wall-Strengthen	2019/2/5	2019/2/11	Strengthen	3941	3706	134
22	F5-Wall-Strengthen	2019/2/11	2019/2/17	Strengthen	8374	8103	294
23	F6-Wall-Strengthen	2019/2/17	2019/2/19	Strengthen	164	91	3
Total		2018/11/16	2019/2/19	——	221669	253836	9775

Table 9 Costs and time for the repair schemes A and B

Repair scheme	Labor cost (CNY)	Material cost (CNY)	Equipment cost (CNY)	Total cost (CNY)	Time (Day)
A	202,210	214,300	9,273	425,783	95
B	221,669	253,836	9,775	485,280	96

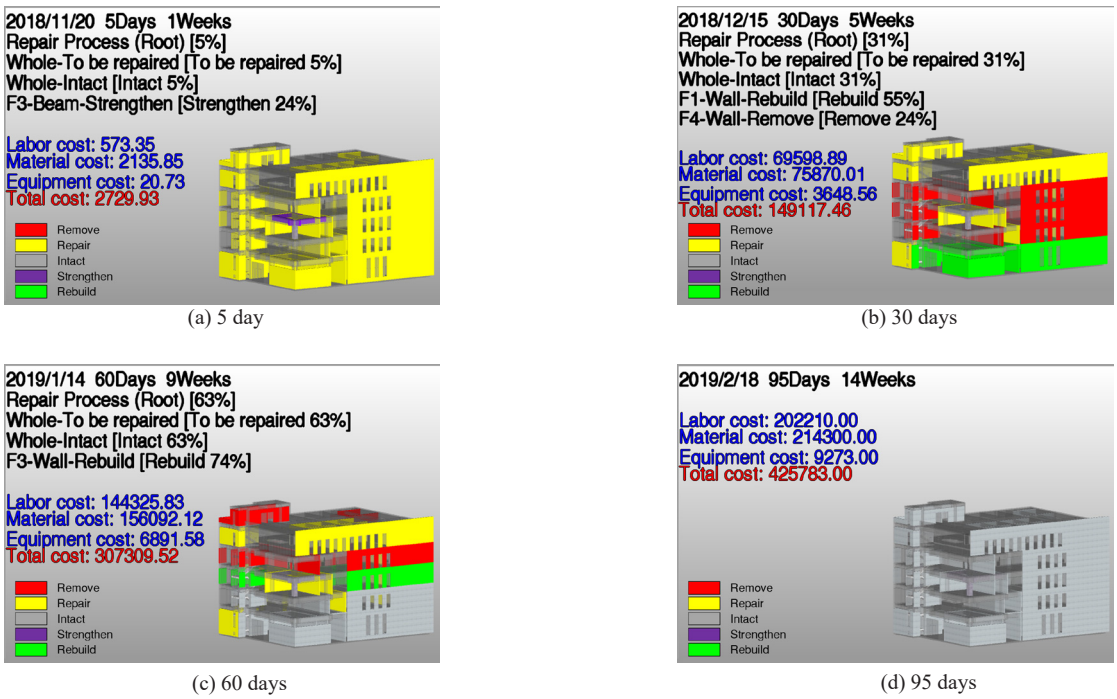

(a) 5 day (b) 30 days

(c) 60 days (d) 95 days

Fig. 16 Different states during post-earthquake repair process

Repair cost and time are important indexes for resilience, which indicate the cost and downtime on seismic resilience. By the proposed method in this study, the detailed repair cost and time were quantified for the repair schemes A and B. By comparing these two repair schemes, it can be found that different repair schemes have significant influence on the seismic resilience of damaged buildings. The proposed method can quantify such influence, which helps the decision makers choose the optimal repair scheme for better seismic resilience

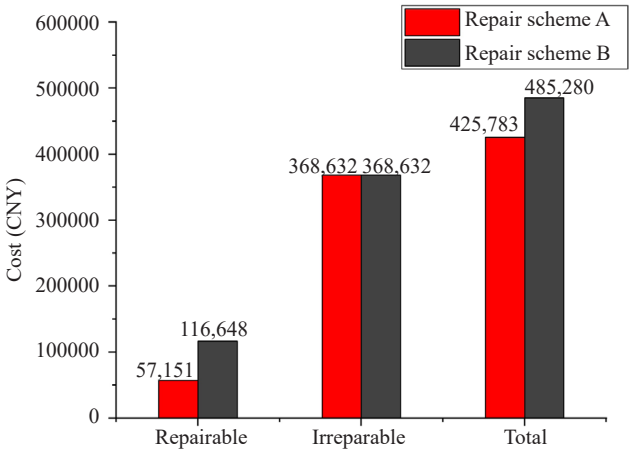

Fig. 17 Repair costs of the repair schemes A and B

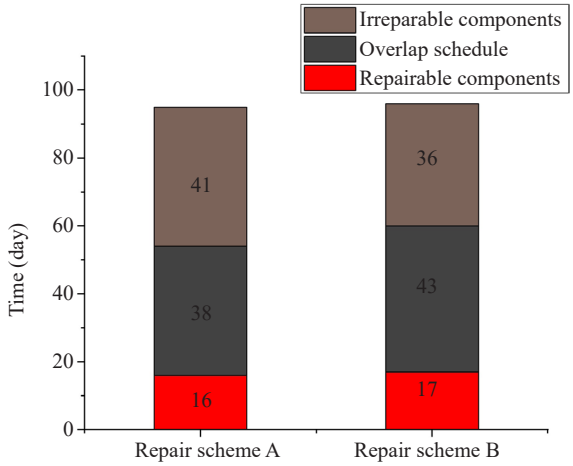

Fig. 18 Repair time of the repair schemes A and B

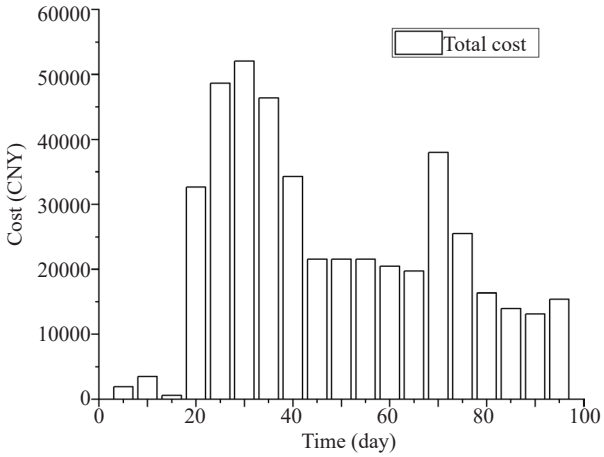

Fig. 19 The total cost at different stages of repair process

of buildings.

In addition, the proposed 5D simulation can also give more detailed results, such as dynamic cost during the repair process. The statistical chart of total costs at different stages is as shown in Fig. 19. From Fig. 19, it can be found that the total cost has a "mountain" distribution during the repair process, which means that

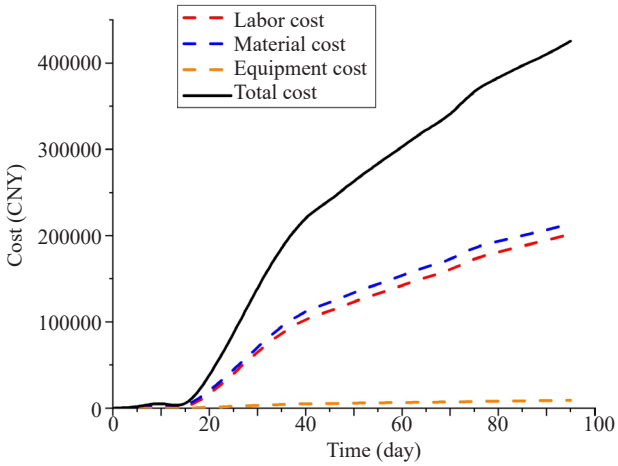

Fig. 20 Cumulating curves of the labor, material, equipment and total costs

the required costs are low at the start and end stages, but high at the middle stage.

Figure 20 shows the cumulating curves of the labor, material, equipment and total costs versus time. It indicates that labor cost and material cost are the main costs of the repair process, while the equipment cost accounts for a relatively low proportion. Such a result is useful for making an accurate plan of cost management for the post-earthquake repair project.

The 5D simulation of the repair process not only presented the repair animation in a 3D realistic way, but also provided the changing process of the detailed costs during the repair period. Such detailed simulation results present the dynamic requirements of labor, equipment and material during the repair process, which are critical to discovering the key repair requirements. By optimizing the key repair requirements, the repair process may be shortened and the resilience of buildings can be thus improved. Therefore, the 5D simulation of the post-earthquake repair process can also benefit decision making in building seismic resilience.

5 Conclusion

A 5D simulation method on the post-earthquake repair process of buildings based on BIM was proposed, and a case study of the 5D simulation of a six-story office building was demonstrated. Some conclusions were drawn as follows:

(1) Through the proposed decision-making model of repair schemes based on the interval index of possibility degree, the optimal repair schemes can be determined for all the damaged components in a building.

(2) By using the designed algorithm for automatic creation of repair schedule, the parameters of the separate flow-repetitive construction can be calculated and therefore the detailed repair schedule can be automatically created.

(3) Through the 5D simulation of the post-earthquake

repair process, the components and the corresponding procedures can be automatically mapped, which saves much manual work. Furthermore, the animation of repair process can be presented in 3D realistic way and the changing details of the costs during repair process can be also displayed.

(4) The proposed 5D simulation method can evaluate building seismic resilience by quantifying repair cost and time. In the case study, the proposed method saved 12.26% of the total cost compared with traditional repair schemes. Furthermore, the proposed method also can provide detailed guidance over the repair process, which benefits the decision making in building seismic resilience.

It is noted that only structural components are investigated in this study, and nonstructural components (e.g., windows, doors, and mechanical, electrical & plumbing (MEP) components) are not yet considered. Actually, the framework and methods of this study are also suitable for nonstructural components, if their seismic damage and the corresponding repair schemes are available. In the future, a 5D repair process of a building, including structural and nonstructural components, will be simulated to provide complete guidance for the decision making on resilience.

Acknowledgement

The authors are grateful for the financial support received from Scientific Research Fund of Institute of Engineering Mechanics, China Earthquake Administration (Grant No. 2019EEEVL0501), General Program of the National Natural Science Foundation of China (Grant No. 51978049) and Beijing Nova Program of Science and Technology (Grant No. Z191100001119115).

References

AbouRizk S (2010), "Role of Simulation in Construction Engineering and Management," *Journal of Construction Engineering and Management-Asce*, **136**(10): 1140–1153. https://doi.org/10.1061/(ASCE)CO.1943-7862.0000220.

Aeido Group. About us. http://www.aeido.cn/ (Access on Oct 13, 2018).

Barazzetti L and Banfi F (2017), "Historic BIM for Mobile VR/AR Applications," *Mixed Reality and Gamification for Cultural Heritage*, pp. 271–290. https://doi.org/10.1007/978-3-319-49607-8_10.

Beijing Municipal Commission of Housing and Urban-Rural Development (BCHUD) (2012), "Beijing Repair Code for Building Renovation Projects," *China Architecture Industry Press*, Beijing, China. (ISBN: 1511223552) (in Chinese)

Bruneau M, Chang SE, Eguchi RT, Lee GC, O'Rourke TD, Reinhorn AM, Shinozuka M, Tierney K, Wallace WA and Winterfeldt Dv (2003), "A Framework to Quantitatively Assess and Enhance the Seismic Resilience of Communities," *Earthquake Spectra*, **19**(4): 733-752. https://doi.org/10.1193/1.1623497.

Charalambos G, Dimitrios V and Symeon C (2014), "Damage Assessment, Cost Estimating, and Scheduling for Post-Earthquake Building Rehabilitation Using BIM," In *Proceedings of the 31st International Conference of CIB W78*, Orlando, Florida, USA, 23-25 June, pp. 398–405. https://doi.org/10.1061/9780784413616.050.

Christodoulou S, Vamvatsikos D and Georgiou C (2010), "A BIM-Based Framework for Forecasting and Visualizing Seismic Damage, Cost and Time to Repair," in K. Menzel, R. Scherer, editors, *Proceedings of the European Conference on Product and Process Modelling 2010*, Cork, Ireland, September 14–16, 2010, pp. 33–38. http://citeseerx.ist.psu.edu/viewdoc/download?doi=10.1.1.721.8440&rep=rep1&type=pdf .

Construction Specifications Institute (CSI) and Construction Specifications Canada (CSC) (2016), "MasterFormat-Master List of Numbers and Titles for the Construction Industry," *Builder's Book*, Los Angeles, CA, USA. (ISBN: 9780997462296)

Eid MS and El-Adaway IH (2017), "Sustainable Disaster Recovery Decision-Making Support Tool: Integrating Economic Vulnerability into the Objective Functions of the Associated Stakeholders," *Journal of Management in Engineering*, **33**(2): 04016041. https://doi.org/10.1061/(ASCE)ME.1943-5479.0000487.

Elnashai AS, Gencturk B, Kwon OS, Al-Qadi IL, Hashash Y, Roesler JR, Kim SJ, Jeong SH, Dukes J and Valdivia A (2010), "The Maule (Chile) Earthquake of February 27, 2010: Consequence Assessment and Case Studies," *MAE Center Report*, No. 10–04. http://hdl.handle.net/2142/18212.

Ge LJ, Wang SX and Jiang XY (2016), "A Combined Interval AHP-Entropy Method for Power User Evaluation in Smart Electrical Utilization Systems," *2016 IEEE Power and Energy Society General Meeting (PESGM)*, Boston, MA, pp:1–5. https://doi.org/10.1109/PESGM.2016.7741067.

Goodrum PM, McLaren MA and Durfee A (2006), "The Application of Active Radio Frequency Identification Technology for Tool Tracking on Construction Job Sites," *Automation in Construction*, **15**(3): 292–302. https://doi.org/10.1016/j.autcon.2005.06.004.

Guha-Sapir D, Vos F, Below R and Ponserre S (2011), "Annual Disaster Statistical Review 2010: The Numbers and Trends," *Centre for Research on the Epidemiology of Disasters*, Université catholique de Louvain, Brussels, pp.12, http://www.cred.be/sites/default/files/ADSR_2010.pdf.

Hamledari H, McCabe B, Davari S and Shahi A (2017), "Automated Schedule and Progress Updating of IFC-Based 4D BIMs," *Journal of Computing in Civil*

Engineering, **31**(4): 04017012. https://doi.org/10.1061/(ASCE)CP.1943-5487.0000660.

Hilfert T and König M (2016), "Low-Cost Virtual Reality Environment for Engineering and Construction," *Visualization in Engineering*, **4**(1): 2. https://doi.org/10.1186/s40327-015-0031-5.

Hofer L, Zampieri P, Zanini MA, Faleschini F and Pellegrino C (2018), "Seismic Damage Survey and Empirical Fragility Curves for Churches after the August 24, 2016 Central Italy Earthquake," *Soil Dynamics and Earthquake Engineering*, **111**: 98–109. https://doi.org/10.1016/j.soildyn.2018.02.013.

Hu SQ, Sun BT and Wang DM (2010), "A Method for Earthquake Damage Prediction of Building Group Considering Building Vulnerability Classification," *Key Engineering Materials*, 217–220. https://doi.org/10.4028/www.scientific.net/KEM.452–453.217.

Jahan A, Bahraminasab M and Edwards K (2012), "A Target-Based Normalization Technique for Materials Selection," *Materials and Design*, **35**: 647–54. https://doi.org/10.1016/j.matdes.2011.09.005.

Kalyan T, Zadeh P, Staub-French S, and Froese T (2016), "Construction Quality Assessment Using 3D As-Built Models Generated with Project Tango," *Procedia Engineering*, **145**: 1416–1423. https://doi.org/10.1016/j.proeng.2016.04.178.

Koliou M and Lindt JW (2020), "Development of Building Restoration Functions for Use in Community Recovery Planning to Tornadoes," *Natural Hazards Review*, **21**(2): 04020004. https://doi.org/10.1061/(ASCE)NH.1527-6996.0000361.

Lee G and Kim J (2014), "Parallel vs. Sequential Cascading MEP Coordination Strategies: A Pharmaceutical Building Case Study," *Automation in Construction*, **43**: 170–179. https://doi.org/10.1016/j.autcon.2014.03.004.

Li D, Yi C and Lu M (2017), "Automation of Project Planning and Resource Scheduling on a Rough Grading Project," In *ASCE International Workshop on Computing in Civil Engineering*, pp. 376–383. https://doi.org/10.1061/9780784480847.047.

Lin CC, Wang WC and Yu WD (2008), "Improving AHP for Construction with an Adaptive AHP Approach (A^3)," *Automation in Construction*, **17**(2): 180–187. https://doi.org/10.1016/j.autcon.2007.03.004.

Lin PH and Wang NY (2017), "Stochastic Post-Disaster Functionality Recovery of Community Building Portfolios I: Modeling," *Structural Safety*, **69**: 96–105. https://doi.org/10.1016/j.strusafe.2017.05.002.

Liu GF; Zhou Z and Xu MZ (2018), "Interval Grey Fuzzy Uncertain Linguistic Sets and Their Application to Ranking of Construction Project Risk Factors," *Journal of Highway and Transportation Research and Development,* **12**(2): 73–80. https://doi.org/10.1061/JHTRCQ.0000628.

Longman M and Miles SB (2019), "Using Discrete Event Simulation to Build a Housing Recovery Simulation Model for the 2015 Nepal Earthquake," *International Journal of Disaster Risk Reduction*, **35**: 101075. https://doi.org/10.1016/j.ijdrr.2019.101075.

Lounis Z and McAllister TP (2016), "Risk-Based Decision Making for Sustainable and Resilient Infrastructure Systems," *Journal of Structural Engineering-Asce*, **142**(9): F401 6005. https://doi.org/10.1061/(ASCE)ST.1943-541X.0001545.

Lu Q, Won J and Cheng JCP (2016), "A Financial Decision Making Framework for Construction Projects Based on 5D Building Information Modeling (BIM)," *International Journal of Project Management*, **34**(1): 3–21. https://doi.org/10.1016/j.ijproman.2015.09.004.

Ministry of Housing and Urban-Rural Development of the People's Republic of China (MOHURD) (2009), "Labour Productivity Standards for Construction Works," *China Planning Press*, Beijing, China. (ISBN: 9788017717104) (in Chinese)

Mohammadi S, Tavakolan M and Zahraie B (2016), "Automated Planning of Building Construction Considering the Amount of Available Floor Formwork," In *Construction Research Congress*, pp. 2197–2206. https://doi.org/10.1061/9780784479827.219.

Nguyen TH (2005), "Automated Construction Planning for Multi-Story Buildings," In *Construction Research Congress 2005: Broadening Perspectives*, pp. 1–10. https://doi.org/10.1061/40754(183)118.

Park J and Cai H (2015), "Automatic Construction Schedule Generation Method through BIM Model Creation," *2015 International Workshop on Computing in Civil Engineering*, pp. 620–627. https://doi.org/10.1061/9780784479247.077.

Powell GH and Allahabadi R (1988), "Seismic Damage Prediction by Deterministic Methods: Concepts and Procedures," *Earthquake Engineering & Structural Dynamics*, **16**(5): 719–734. https://doi.org/10.1002/eqe.4290160507.

Scheuer C, Keoleian G and Reppe P (2003), "Life Cycle Energy and Environmental Performance of a New University Building: Modeling Challenges and Design Implications," *Energy and Buildings*, **35**(10): 1049–1064. https://doi.org/10.1016/S0378-7788(03)00066-5.

Tauscher E, Smarsly K, König M and Beucke K (2014), "Automated Generation of Construction Sequences Using Building Information Models," In *Proceedings of the 31st International Conference of CIB W78*, Orlando, Florida, USA, 23–25 June, pp. 745–752. https://doi.org/10.1061/9780784413616.093.

Torres-Calderon W, Chi Y, Amer F and Golparvar-Fard M (2019), "Automated Mining of Construction Schedules for Easy and Quick Assembly of 4D BIM Simulations," In *ASCE International Conference on Computing in Civil Engineering 2019: Visualization,*

Information Modeling, and Simulation, I3CE 2019, pp. 432–438. https://doi.org/10.1061/9780784482421.055.

Wan SP and Dong JY (2014), "A Possibility Degree Method for Interval-Valued Intuitionistic Fuzzy Multi-Attribute Group Decision Making," *Journal of Computer and System Sciences*, **80**: 237–256. https://doi.org/10.1016/j.jcss.2013.07.007.

Wang B and Liu J (2019), "Comprehensive Evaluation and Analysis of Maritime Soft Power Based on the Entropy Weight Method (EWM)," *Journal of Physics: Conference Series*, **1168**. https://doi.org/10.1088/1742-6596/1168/3/032108.

Wang S (2013), "Integrated Digital Building Delivery System Based on BIM and VR Technology," *Applied Mechanics and Materials*, pp. 3193–3197. https://doi.org/10.4028/www.scientific.net/AMM.380-384.3193.

Wang YM, Yang JB and Xu DL (2005), "A Two-Stage Logarithmic Goal Programming Method for Generating Weights from Interval Comparison Matrices," *Fuzzy Sets and Systems*, **152**(3): 475–498. https://doi.org/10.1016/j.fss.2004.10.020.

Wen Y (2015), "Research on Cost Control of Construction Project Based on the Theory of Lean Construction and BIM: Case Study," *The Open Construction and Building Technology Journal,* **8**(1): 382–88. https://doi.org/10.2174/1874836801408010382.

Wu YH, Zhu W, Li XQ and Gao R (1995), "Interval Approach To Analysis of Hierarchy Process," *Journal of Tianjin University*, **1995**(05): 700–705. https://kns.cnki.net/kcms/detail/detail.aspx?FileName=TJDX505.021&DbName=CJFQ1995. (in Chinese)

Xiong C, Lu XZ, Lin XC, Xu Z and Ye LP (2017), "Parameter Determination and Damage Assessment for THA-Based Regional Seismic Damage Prediction of Multi-Story Buildings," *Journal of Earthquake Engineering*, **21**(3): 461–485. https://doi.org/10.1080/13632469.2016.1160009.

Xiong C, Huang J and Lu XZ (2020), "Framework for City-Scale Building Seismic Resilience Simulation and Repair Scheduling with Labor Constraints Driven by Time-History Analysis," *Computer-Aided Civil and Infrastructure Engineering*, **35**(4): 322–341. https://doi.org/10.1111/mice.12496**.**

Xu J (2017), "Research on Application of BIM 5D Technology in Central Grand Project," *Procedia Engineering*, **174**: 600–610. https://doi.org/10.1016/j.proeng.2017.01.194.

Xu Z, Zhang HZ, Lu XZ, Xu YJ, Zhang ZC and Li Y (2019), "A Prediction Method of Building Seismic Loss Based on BIM and FEMA P-58," *Automation in Construction*, **102**: 245–257. https://doi.org/10.1016/j.autcon.2019.02.017.

Yang YM, Peng JX, Cai CS and Zhang JR (2019), "Improved Interval Evidence Theory–Based Fuzzy AHP Approach for Comprehensive Condition Assessment of Long-Span PSC Continuous Box-Girder Bridges," *Journal of Bridge Engineering*, **24**(12): 04019113. https://doi.org/10.1061/(ASCE)BE.1943-5592.0001494.

Ye J (2015), "Multiple Attribute Decision-Making Method Based on the Possibility Degree Ranking Method and Ordered Weighted Aggregation Operators of Interval Neutrosophic Numbers," *Journal of Intelligent and Fuzzy Systems*, **28**(3): 1307–1317. https://doi.org/10.3233/IFS-141416.

Yeoh JKW, Nguyen TQ and Abbott ELS (2017), "Construction Method Models Using Context Aware Construction Requirements for Automated Schedule Generation," In *ASCE International Workshop on Computing in Civil Engineering 2017*, pp. 60–67. https://doi.org/10.1061/9780784480847.008.

Yu YX and Zheng ZH (2004), "Application of Paterkovsky Method in Organizing Non-rhythmic Flowing Water Construction," *Shanxi Architecture*, **30**(18): 90–91. https://doi.org/10.13719/j.cnki.cn14-1279/tu.2004.18.057. (in Chinese)

Yue JG, Qian J and Beskos DE (2016), "A Generalized Multi-Level Seismic Damage Model for RC Framed Structures," *Soil Dynamics and Earthquake Engineering*, **80**: 25–39. https://doi.org/10.1016/j.soildyn.2015.10.005.

Yun SH, Jun KH, Son CB and Kim SC (2014), "Preliminary Study for Performance Analysis of BIM-Based Building Construction Simulation System," *Ksce Journal of Civil Engineering*, **18**(2): 531–540. https://doi.org/10.1007/s12205-014-0174-2.

Zhou Y, Ding LY, Wang XY, Truijens M and Luo HB (2015), "Applicability of 4D Modeling for Resource Allocation in Mega Liquefied Natural Gas Plant Construction," *Automation in Construction*, **50**: 50–63. https://doi.org/10.1016/j.autcon.2014.10.016.

Zhu BQ and SongWX (2016), "Study on the Flow Construction," *Journal of Anyang Institute of Technology*, **15**(02): 51–53. https://doi.org/10.19329/j.cnki.1673-2928.2016.02.014. (in Chinese)